



Surface and bulk electron irradiation effects in simple and complex glasses



Anamul H. Mir^{a,*}, B. Boizot^b, T. Charpentier^c, M. Gennisson^a, M. Odorico^d, R. Podor^d, C. Jégou^a, S. Bouffard^e, S. Peugeot^{a,*}

^a CEA, DEN, DTCD, SECM, LMPA, BP 17171, 30207 Bagnols-sur-Cèze Cedex, France

^b Laboratoire des Solides Irradiés, UMR 7642 CEA-CNRS-Ecole Polytechnique, 91128 Palaiseau, France

^c CEA, CNRS, Université Paris-Saclay, CEA, Saclay 91191, Gif-sur-Yvette, France

^d ICSM – UMR 5257 CEA-CNRS-UM-ENSCM, 30207 Bagnols-sur-Cèze Cedex, France

^e CIMAP-GANIL (CEA-CNRS-ENSCAEN-Univ. Caen), BP 5133, 14070 Caen Cedex 5, France

ARTICLE INFO

Article history:

Received 23 July 2016

Received in revised form 5 October 2016

Accepted 6 October 2016

Available online 12 October 2016

Keywords:

Electron irradiation

Glasses

Radiation damage

ToF-SIMS

Raman spectroscopy

ABSTRACT

A three oxide sodium borosilicate (BS3) and a complex, thirty oxide borosilicate glass (SON68) were irradiated with 2.3 MeV electrons to doses ranging from 0.15 GGy to 4.6 GGy at 350 K. The irradiated glasses were characterized using Raman and NMR spectroscopies, ToF-SIMS, AFM and microhardness to understand surface and bulk irradiation effects. Glass surfaces were observed to be depleted of the alkali atoms. The depletion depth depended on the dose and glass composition, reaching 660 nm and 500 nm on any vacuum facing surface for BS3 and SON68 at 4.6 GGy respectively. The alkali-depleted region was enriched in molecular oxygen and showed characteristics of phase separated glasses. In the bulk of the glass, Raman and NMR spectroscopies showed a silica network depolymerisation, a transformation of 4 to 3-coordinated boron and formation of non-bridging oxygen atoms on silicon and boron atoms. The hardness of the depolymerized glasses decreased by 20% (BS3) and 10% (SON68). Based on the experiments and theory, it is shown that electron stimulated desorption is the dominant surface depletion mechanism. These results show that the surfaces behave differently than the bulk of the glass. Therefore, surface related phenomena are expected to be dominant in TEM and other in-situ and ex-situ surface characterizations having depth resolution of a few hundred nanometers. Thus, sample size plays an important role in evaluating the radiation damage and one must be careful in extending the conclusions drawn from surface sensitive techniques to bulk irradiation effects in electron irradiated glasses.

© 2016 Elsevier B.V. All rights reserved.

1. Introduction

Nuclear waste glass matrices confining minor actinides and fission products are subjected to self-irradiation damage due to alpha and beta decays. The major alpha-emitting radionuclides are Cm²⁴⁴, Am²⁴¹, Am²⁴³, Np²³⁹, Np²³⁷, Pu²³⁹ and Pu²⁴⁰; whereas Cs¹³⁷, Sr⁹⁰, Y⁹⁰, Pm¹⁴⁷, and Cs¹³⁴ are the major beta emitting radionuclides (see Fig. S1 in the Supplementary Material (SM) [1]). Due to the short half-life time of all these beta radionuclides and some of the alpha emitters (Cm²⁴⁴ and Am²⁴¹), the waste matrices can experience temperatures between 570 and 370 K during first few hundred years of the disposal because of the intense dose rate. After this, the long-lived alpha emitters are the main radiation source and the temperature is relatively low, mainly controlled by the repository conditions.

In order to evaluate and understand the impact of beta decays on different glass properties that might occur mainly over first few hundred years, model glass compositions are externally irradiated with electron beams to simulate the beta decay damage. Two commonly used approaches are: (i) in-situ characterization and irradiation of few tens to few hundred nanometer thin films with keV range electrons in a TEM and (ii) irradiation of thick samples in a high energy electron accelerator.

The first approach usually involves fluxes in the range of 10¹⁵ electrons·cm⁻²·s⁻¹ to 10²⁰ electrons·cm⁻²·s⁻¹ [2–6] allowing to attain very high doses (up to a few hundred GGy) in a short time span (minutes to hours). Under such conditions, borosilicate glasses undergo boron coordination changes (tetrahedral BO₄ to trigonal BO₃ transformation) and phase separation [2–5,7] driven by alkali migration (the rate of the migration is inversely proportional to the alkali mass [8]). Oxygen bubbles have also been observed in some cases [4,9]. However, the final fate of the alkali atoms is not very well understood and established.

The second approach involves irradiation with high energy electron accelerators in which thick and large samples can be used. This makes it

* Corresponding authors.

E-mail addresses: mirinamulhaq@gmail.com (A.H. Mir), sylvain.peuget@cea.fr (S. Peugeot).

possible to use multiple structural and macroscopic characterization tools on post-irradiated samples. Studies are usually carried out with fluxes that are about two to three orders of magnitude lower than the lowest studied fluxes in TEM's. Therefore, it is difficult to attain very high doses and studies are usually limited to few Giga-Grays only. Under such conditions, Raman spectroscopy has revealed the formation of molecular oxygen [10–13] in addition to some other structural changes, like a decrease in the Si—O—Si bond angle and a change in the degree of polymerization [12–15]. In addition, a decrease in the hardness and elastic modulus has also been observed [14,16].

When comparing TEM and accelerator based studies, it is important to bear in mind that TEM and various in-situ characterizations employed therein provide an idea about the changes occurring in a very thin layer of the glass, whereas bulk characterizations employed on thick samples irradiated in electron accelerators can provide an idea about the radiation damage in the bulk glass volume that is not exposed to the vacuum. Whether the two approached can converge or not is debatable and will be discussed in this work.

Despite many studies with low and high energy electrons, there are some critical and fundamental questions listed below that have not been addressed so far and are the focus of our research: (i) How different are the near surface electron irradiation effects from the one occurring in the bulk of the glass? And how different characterizations with different spatial resolutions can shed light on this aspect, and (ii) How relevant are the TEM-based studies using thin samples with very large surface to volume ratio for understanding the bulk irradiation effects and addressing the irradiation damage in nuclear waste glass matrices?

Therefore, the focus of this study is to provide an in-depth understanding of the electron irradiation effects occurring at the sample surface and in the bulk of the glass. For this purpose simple and complex borosilicate glass were irradiated with 2.3 MeV electrons to various doses up to about 4.6 GGy. The samples were characterized using MAS NMR and Raman spectroscopy for structural changes, micro-hardness for changes in the mechanical properties, and AFM and ToF-SIMS for surface modification and surface composition changes.

2. Samples and electron irradiation

Prior to the electron irradiation, all six faces ($6 \times 6 \times 0.5 \text{ mm}^3$) of the BS3 and SON68 glass samples were optically polished (see SM [1] for the glass compositions). The samples were annealed at around $T_g + 20$ ($T_g = 875 \text{ K}$ for BS3 and 775 K for SON68) for about 15 min. The annealing was done to remove any stresses from the polishing and reduce the surface roughness from 2 nm to $<1 \text{ nm}$ (low surface roughness is important for secondary ion mass spectroscopy and AFM). For irradiation, two samples stacked together were wrapped in a $20 \mu\text{m}$ thick copper foil and then held in place by screwing a $100 \mu\text{m}$ thick copper foil on top of the sample holder (See Fig. S2 in the SM [1]). The irradiation was performed at a flux of about $5 \times 10^{13} \text{ electrons} \cdot \text{cm}^{-2} \cdot \text{s}^{-1}$ at the SIRIUS irradiation facility (Laboratoire des Solides Irradiés, Ecole Polytechnique, France) at a temperature of about 350 K (under 400 mbar helium atmosphere). The energy of the initial 2.5 MeV electrons (1 cm beam radius) after passing through an overall thickness of about $120 \mu\text{m}$ copper foil was reduced to 2.3 MeV (see Fig. S3 in the SM [1]). Doses of $0.15, 0.87, 1.4, 3.14,$ and 4.57 GGy were studied. The samples were fully covered by the beam cross section (3.14 cm^2) and homogeneously irradiated.

3. Characterizations and results

3.1. Confocal Raman spectroscopy

Horiba HR800 micro-Raman spectrometer using 532 nm excitation laser (green) and the $100\times$ objective was used for non-polarized confocal Raman spectroscopy. The depth, lateral and spectral resolution were $1.6 \mu\text{m}$, $1 \mu\text{m}$, and 1.7 cm^{-1} respectively. The spectra were acquired at different locations on the $6 \text{ mm} \times 6 \text{ mm}$ faces (referred as major faces/

top and bottom faces) and on the $6 \text{ mm} \times 0.5 \text{ mm}$ faces (referred as minor faces/bordering faces) as shown in Fig. 1 to study the spatial variation of the damage. On each surface, the spectra were taken from $+x$ to $-x$ and $+y$ to $-y$ going through the centre of the face. For the sake of brevity, the detailed results are shown for the highest dose sample only (4.57 GGy) and the results of lower dose samples which follow a similar trend are shown in the Supplementary figures in SM [1].

The Raman spectra acquired at different positions on one of the major surfaces are shown in Fig. 2(a) and the Raman spectra (O_2 profiles only; peak at 1552 cm^{-1}) acquired along vertical and horizontal directions on one of the minor faces are shown in Fig. 2(b).

The Raman spectra in Fig. 2(a, b) show that the electron irradiation resulted in the formation of molecular oxygen (1552 cm^{-1} peak [17]). The intensity of the molecular oxygen peak was found to be maximum in the centre of the faces (major and minor). The intensity decreased in moving away from the centre towards the edges and the edges did not show any signs of the O_2 formation. Note that the region within a distance of $10 \mu\text{m}$ from the border is defined as the edge in the present context. Therefore, unlike the central regions of the surfaces, the region extending at least up to about $10 \mu\text{m}$ from the edges did not contain any O_2 . The decrease in the oxygen intensity signal was almost symmetric with respect to the centre of the faces (i.e. drops symmetrically in $\pm x$ and $\pm y$). The region from 850 cm^{-1} to 1250 cm^{-1} referred as Q^n region [18–20] (n represents the number of bridging oxygen atoms and $0 \leq n \leq 4$) gives an idea of the silica network connectivity (in a fully polymerized network, each silicon atom is connected to the rest of the glass network through four oxygen atoms called as bridging oxygen atoms). The structural units with a high degree of polymerization contribute towards the high-frequency side of the Q^n region and the units with a low degree of polymerization contribute towards the low-frequency side. A relative decrease in the intensity on the high-frequency side ($>1140 \text{ cm}^{-1}$) and an increase in the mid-frequency ($>1050 \text{ cm}^{-1}$) and low-frequency side ($<1050 \text{ cm}^{-1}$) indicate a network depolymerisation. This will be discussed later in more detail. However, the spectra near the centre showed a more pronounced increase in the low-frequency side peak at 940 cm^{-1} (see spectra from $+2.4 \text{ mm}$ to -2.4 mm . Note that a peak near 930 cm^{-1} to 940 cm^{-1} is observed in $\text{SiO}_2 \cdot \text{B}_2\text{O}_3$ system. See Fig. 2 in [21]) The intensity of the 630 cm^{-1} band (Danburite units; four-coordinated boron surrounded by three silicon atoms and one boron atom [22–24]) showed a relatively large decrease in the intensity near the centre of the faces. The frequency of the broad band near 490 cm^{-1} (R band) which gives an idea about the average Si—O—Si bond angle also changed. The edges showed an increase in the position of the R band by about 6 cm^{-1} whereas the central regions of the sample showed a decrease by about 3 cm^{-1} (see Section-2 in the SM regarding the determination of R band position).

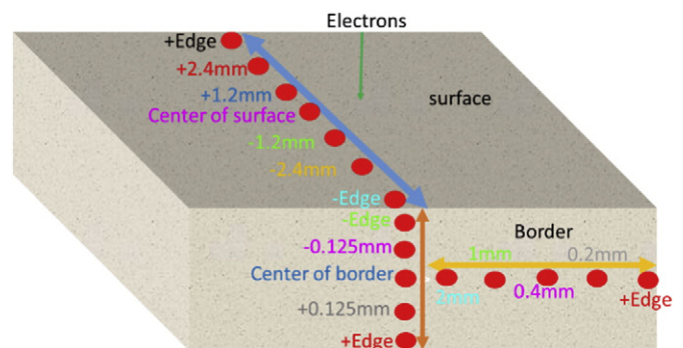


Fig. 1. The locations of Raman spectra acquisition. The spectra were acquired on all six faces from $+x$ to $-x$ and $+y$ to $-y$ going through the centre of the faces. The $6 \text{ mm} \times 6 \text{ mm}$ faces (top and bottom) will be referred as major faces and $6 \text{ mm} \times 0.5 \text{ mm}$ faces (bordering faces) will be referred as minor faces in the subsequent manuscript. At a given location, spectra were also acquired in the immediate neighbourhood to look for any damage inhomogeneities.

Download English Version:

<https://daneshyari.com/en/article/5441561>

Download Persian Version:

<https://daneshyari.com/article/5441561>

[Daneshyari.com](https://daneshyari.com)